Meyer-Neldel rule in the conductivity of manganite single crystals

J. Przybytek,[1,2,*] V. Markovich,[3] and G. Jung[3,4]
[1]*Institute of High Pressure Physics, Polish Academy of Sciences, 01-142 Warsaw, Poland*
[2]*Institute of Experimental Physics, Faculty of Physics, University of Warsaw, 02-093 Warsaw, Poland*
[3]*Department of Physics, Ben Gurion University of the Negev, 84105 Beer Sheva, Israel*
[4]*Institute of Physics, Polish Academy of Sciences, 02-668 Warsaw, Poland*

(Received 28 May 2018; revised manuscript received 27 July 2018; published 28 September 2018)

The Meyer-Neldel behavior of conductivity of low-doped manganite $La_{1-x}Ca_xMnO_3$ single crystals has been investigated. The evolution of the isokinetic temperature of conductivity, modified by Ca-doping, hydrostatic pressure, and current bias has been determined. In addition, the evolution of isokinetic temperature with ageing has also been studied. The Meyer-Neldel behavior of the manganite system stems from the multiexcitation entropy mechanism. The isokinetic temperature turned out to be a sensitive parameter characterizing changes in the transport properties of mixed valence manganites, which in the presence of a detailed theoretical model of the excitations coupling in manganites could become a powerful tool for the characterization and investigation of transport properties of manganites.

DOI: 10.1103/PhysRevB.98.115159

I. INTRODUCTION

The Meyer-Neldel rule is an empirical relation, originally derived in chemical kinetics almost a century ago, stating that the enthalpy and entropy of a chemical reaction are proportional to each other. Since then, the phenomenon, also referred to as the compensation law, the isokinetic rule, or the Meyer-Neldel rule (MNR), was observed in many processes in chemistry, condensed matter physics, biology, and geology [1].

Meyer and Neldel determined that in the thermally activated electrical conductivity of some oxide semiconductors the pre-exponential temperature independent factor of the conductivity increases exponentially in proportion to the thermal activation energy. In more general terms, MNR states that the decrease of the rate of a thermally activated process, due to a change in the activation energy, can be partially compensated by an opposite change of the pre-exponential factor. In the case of thermally activated electrical resistivity,

$$\rho(T) = \rho_0 \exp(-E_a/k_B T), \tag{1}$$

a resistivity change due to the change of the activation energy barrier can be compensated by a change of the pre-exponential factor ρ_0,

$$\rho(T) = \rho_{00} \exp(E_a/k_B T_{\mathrm{MN}}) \exp(-E_a/k_B T), \tag{2}$$

where ρ_{00} is a constant of a given process and T_{MN} stands for the isokinetic or Meyer-Neldel temperature.

The comprehensive theoretical explanation of the compensation effect in a variety of physical systems was not available for a long time. At present, there are two types of theoretical models explaining the MNR effect in the solid state: the statistical shift models and the multiexcitation entropy models [1].

In the statistical shift of the Fermi (SSF) level models, disorder causes an asymmetry between the density of states (DOS) above and below the Fermi level. The Fermi level shifts with temperature. Since thermally activated charge-carriers hop from the Fermi level to the mobility edge, the DOS asymmetry causes the activation barriers to change with temperature as well, which leads to a compensation effect. The isokinetic compensation temperature in the SSF model is directly related to the disorder in the system, namely to the width of the DOS distribution. For an exponential DOS distribution, $T_{\mathrm{MN}} = E_w/k_B$, where E_w is the width of the distribution. The SSF models cannot, however, properly explain the MNR in several systems, in particular in those with large activation energies. Therefore it is now assumed that SSF models describe properly only the "apparent," rather than a genuine MNR effect [2–4].

The more general multiexcitation entropy (MEE) thermodynamic models, which apply also to nonsolid state systems, take into account that the kinetic behavior of a system depends on the free energy rather than on the energy or the enthalpy alone. When an activation energy is large, the thermally activated process needs to acquire a big number of individual excitations to overcome a barrier. A large number of activations can be assembled out of the total number of available excitations in many ways, which increases the entropy $S = k_B \ln W$, where W is the number of microscopically different states giving rise to the same macroscopic thermodynamic state. The activation entropy becomes proportional to the enthalpy and leads to MNR behavior.

Equation (2) has in fact a form of the Eyring equation,

$$\begin{aligned}\rho(T) &= \rho_0 \exp(-\Delta G/k_B T) \\ &= \rho_{00} \exp(\Delta S/k_B) \exp(-\Delta H/k_B T),\end{aligned} \tag{3}$$

where $G = H - TS$ stands for the free energy, S for entropy, and H for enthalpy. Assuming that the acquired elementary

*jacek.przybytek@fuw.edu.pl

excitations are identical, as is in the case of phonons in a solid state system, the number of excitations necessary to pass the barrier is $n = \Delta H/\hbar\omega_0$, where $\hbar\omega_0$ is the energy of each individual phonon excitation. In the limit of large number of excitations n, ΔS becomes proportional to ΔH, and the characteristic Meyer-Neldel temperature is [1]

$$T_{\mathrm{MN}} = \frac{\hbar\omega_0}{k_B \ln N}, \tag{4}$$

where N is a coupling constant measuring the number of available excitations within an interaction volume. Thus, whenever the activation energy is large with respect to thermal excitations, the kinetic compensation, namely the MNR behavior should appear [1].

The general concept of multiexcitation kinetics has to be adapted to the physics of each particular system to fully understand the mechanisms involved and the physical meaning of the isokinetic temperature. For example, Emin has showed that the multiexcitation processes result in MNR behavior of the hopping conductivity of polarons [5]. In the semiclassical adiabatic polaron hopping regime, charge transfer occurs when electronic energy levels of carriers are brought into temporary coincidence. Without rapid dissipation of the vibrational energy, an adiabatic hop is followed by a return hop. Back and forth motion of an activated state lowers the frequencies of the associated atom vibrations and increases the entropy of the activated state. The entropy increase lowers the activation energy, the minimum energy required to achieve a coincidence, which enhances the thermally activated rate of hopping. The proportionality between additional entropy and the hopping activation energy results in the MNR effect in the hopping conductivity [5].

In experiments, by varying a parameter that changes the activation energy and thus influences the rate of a thermally activated process, one may investigate how the pre-exponential factor from Eq. (1) varies with the activation energy and determine the value of the isokinetic temperature T_{MN} from the slope of a linear dependence of the logarithm of the pre-exponential factor on the activation energy. It follows from Eq. (2) that thus determined temperature $T = T_{\mathrm{MN}}$ should be consistent with the temperature at which the process becomes independent of the parameter that changes the activation energy.

Meyer-Neldel behavior in electrical conductivity was reported for several strongly disordered systems. Among them, narrow-band inorganic semiconductors, organic semiconductors, noncrystalline semiconductors, nonmetallic $YBa_2Cu_3O_y$, fullerenes, and a wide range of chalcogenide glasses [1]. However, there is no reason why MNR should be limited to the above materials. Indeed, according to the MEE model, MNR should appear whenever the activation energy is large compared with the excitations of the system and the thermal energy. Nevertheless, we are not aware of any report of MNR in ordered crystalline materials. In particular, to our best knowledge, there are no reports on MNR in the conductivity of bulk single crystals of mixed valence manganites. At present, we are aware of only one paper on MNR in the low bandwidth colossal magnetoresistive thin films of $Pr_{0.68}Ca_{0.32}MnO_3$ manganite with different degrees of octahedral disorder [6].

One of the characteristic features of mixed valence manganites is a pronounced dynamic phase separation (PS), consisting in the coexistence of phases with different orbital order and electronic properties. One of the consequences of such strong PS in low-doped $La_{1-x}Ca_xMnO_3$ (LCMO) manganites is the appearance of peculiar metastable states with different resistivities [7–11]. The metastable states are characterized, among others, by pronounced low-frequency conductivity fluctuations. The noise is typically of the $1/f$ type but it frequently exhibits also non-Gaussian and nonequilibrium features [12–15]. The non-Gaussian component of the noise usually appears as random telegraph noise (RTN), in which the conductivity randomly jumps between two fixed "up" and "down" levels, while the lifetimes at each of the levels are exponentially distributed.

Recently, we have reported on a robust RTN appearing in a very wide temperature range in the low-resistivity metastable state of freshly grown $La_{0.86}Ca_{0.14}MnO_3$ single crystals [15]. We have concluded that the mechanism responsible for such conductivity fluctuations is dynamic current redistribution, consisting in thermally activated switching between different current flow patterns, assisted by a particular feedback mechanism. We will demonstrate in this paper that the feedback stems from the MNR behavior of the current-dependent resistivity.

In the rich phase diagram of hole-doped LCMO manganites, $x < 0.5$, the critical doping level $x_c = 0.225$ separates the ferromagnetic and metallic (FMM) ground state above x_c from the orbital ordered ferromagnetic insulating (FMI) ground state below x_c. At hole-doping level $x < 0.125$, the ground state of LCMO becomes insulating and antiferromagnetic. In the entire doping range $0.125 < x < 0.225$, an additional insulating ferromagnetic phase, incompatible with the double exchange mechanism, coexists with the ferromagnetic metallic phase and strongly influences the electrical conductivity of LCMO manganites [16]. With increasing temperature, the FMM phase undergoes a concomitant metal-to-insulator and FM-to-paramagnetic transitions.

The transport properties of doped perovskite manganites can be modified by changing the external factors, such as magnetic field, electric fields, hydrostatic pressure, electromagnetic irradiation, and electric current [17]. Nevertheless, the primary factor influencing the conductivity of low-Ca-doped LCMO manganites is the Ca-doping level x [18].

In this paper, we discuss comprehensive investigations of Meyer-Neldel behavior of the electrical conductivity of low-Ca-doped LCMO bulk single crystals in which we have varied the conductivity by means of doping, hydrostatic pressure, dc current flow, and ageing.

II. EXPERIMENTAL

LCMO single crystals with various doping levels x were grown from sintered ceramic rods of high-purity commercial La_2O_3, $CaCO_3$, and MnO_2 precursors by means of the floating zone technique. To account for the Ca segregation coefficient, which is smaller than one, and to compensate for the evaporation of manganese during the crystallization process, the starting rods had slight excess of Ca and Mn content. The crystals were grown in air, using a double mirror 2.5 kW

high-pressure Xenon lamp optical furnace. Previously grown single crystals were used as seeds. The speed of growth was 2.5 mm/h and the feed rod and the seed crystal were rotated in opposite directions with a rate of 10–20 rpm.

Quantitative analysis of the chemical composition was performed on the polished planes of the crystals by field emission scanning electron microscopy. The average chemical composition was checked by scanning electron microscopy and EDX analysis. Phase analysis of the crystals was performed at room temperature by x-ray powder diffraction. The diffraction peaks were indexed in the orthorhombic setting of the *Pnma* space group and the Rietveld analysis of XRD spectrum, was employed to refine the lattice parameters. The detailed results of the structural, chemical, resonance, and magnetic characterization of the employed crystals were published elsewhere [7–9,11,15].

As grown crystals consisted of large randomly oriented blocks. The dominant orientation within the blocks was determined using a four-circle x-ray diffractometer. Samples for the transport measurements were cut off from the areas with well defined orientation and had the form of 1-mm-thick and 3-mm-wide bars directed along the [100] crystalline direction. Current and voltage leads were indium soldered to the vacuum evaporated gold contacts.

Transport characteristics were measured in a standard four-point contact arrangement with 0.33 mm distance between the voltage contacts. Voltages developing across a current biased sample were amplified by a very low-noise room-temperature preamplifier located on the top of the cryostat and processed by a computer. Because of the relatively high impedance of the samples, especially at low temperatures, a particular attention was paid to the level of the signal at the amplifier input to avoid the saturation and not to exceed the allowed common voltage level during data acquisition. The resistivity characteristics were measured using alternatively ac lock-in or dc current techniques.

Measurements of LCMO resistance under hydrostatic pressure were carried out in a CuBe pressure cell. The temperature was measured by copper-constantan thermocouple attached to the cell, while the pressure was monitored by a manganin gauge.

III. RESULTS AND DISCUSSION

A. Doping-dependent conductivity

The Ca-doping level x is the strongest factor influencing the conductivity of mixed valence LCMO manganites. Figure 1 shows the evolution of temperature dependence of the resistivity of LCMO single crystals on the doping level x.

One may notice that the $x = 0.3$ crystal displays a Curie temperature, which is slightly depressed with respect to $T_C \approx$ 250 K, most frequently reported for ceramic samples of this composition [19]. Manganite's Curie temperature is strongly influenced by intrinsic nonmagnetic (chemical) A-site atomic scale disorder, due to size mismatch between trivalent and divalent cations [20]. The high-temperature (1600 °C) floating-zone method, using for growing of the LCMO single crystals is characterized by unavoidable competition of quenching and annealing during cooling time, which results in additional

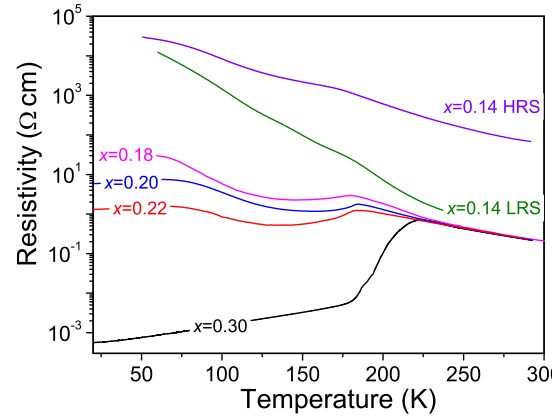

FIG. 1. Temperature dependence of the resistivity of $La_{1-x}Ca_xMnO_3$ single crystals with doping level $x = 0.3$, 0.22, 0.2, 0.18, and 0.14 in high (HRS) and low (LRS) metastable resistivity state.

intrinsic spatial doping inhomogeneity and chemical disorder. This effect is enhanced by a high value of Ca distribution coefficient. Thus the disorder becomes most pronounced at high levels of Ca doping. The combined influence of these factors is responsible for the appearance of spatial fluctuations of the dopant content and the depression of T_C in LCMO [21–23]. The sintering temperatures of LCMO ceramics are significantly lower, making the T_C of LCMO ceramic consistently higher compared to single crystals with the same Ca-doping level.

The ground state of the crystal doped at the highest investigated level $x = 0.3$ is ferromagnetic and metallic. Below the Curie temperature T_C, resistivity sharply and monotonously drops with decreasing temperature. In the paramagnetic temperature range above T_C, the resistance has a semiconducting, thermally activated character. With the doping decreasing below the critical $x_c = 0.225$, the form of $\rho(T)$ characteristics changes. There appears a pronounced resistivity maximum at the metal-insulator (M-I) transition temperature, which coincides, within the experimental error, with the Curie temperature T_C, obtained from independent magnetic measurements. The maximum is followed by a subsequent resistivity upturn at lower temperatures. However, when the doping drops towards the low doping limit of the existence of the ferromagnetic ground state, $x = 0.125$, the maximum at M-I transition practically disappears and only a slight inflexion in the $\rho(T)$ curve is visible at $T = T_C$, as can be seen in Fig. 1 in the $x = 0.14$ recordings.

Labels HRS and LRS in Fig. 1 refer to high- and low-metastable resistivity states. The pristine state of the freshly crystalized $La_{0.86}Ca_{0.14}MnO_3$ was the high-resistivity state. However, during the very first days of experiments involving thermal cycling between liquid He and room temperatures, accompanied by several dc current bias sweeps, the sample spontaneously evolved into the low-resistivity state, as discussed in details in Ref. [11]. The spontaneously created low-resistivity state persisted during three months of subsequent experiments, in which we have observed and characterized, among others, the robust random telegraph noise [15]. After two months break in the experiments, the crystal

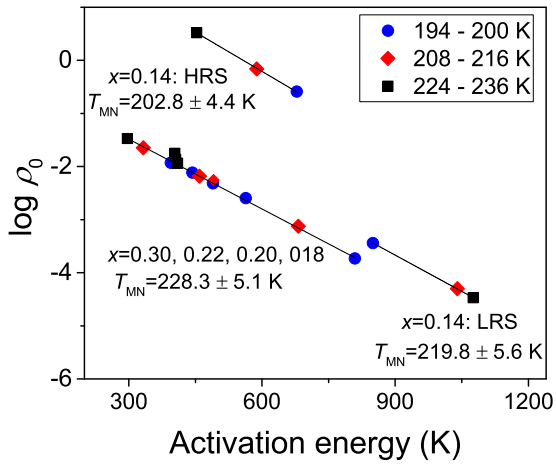

FIG. 2. Dependence of the Arrhenius pre-exponential resistivity factor on the local activation energy for various doping levels. Different symbols refer to different temperature ranges in which Eq. (1) was fitted to $\rho(T)$ data, see the legend. Two resistivity states, HRS- high-resistivity and LRS-low-resistivity metastable states are shown for $x = 0.14$.

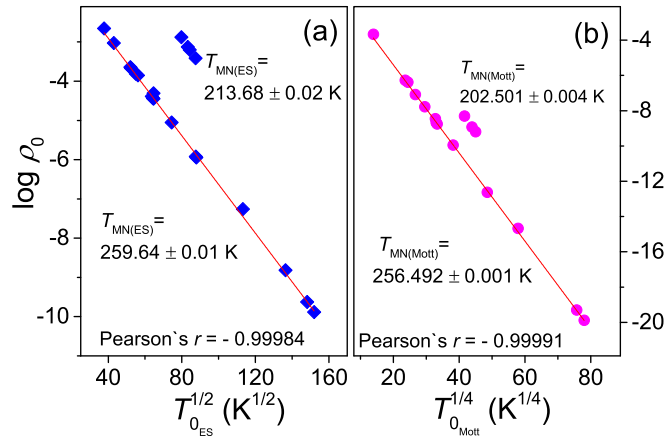

FIG. 3. Dependence of the Arrhenius pre-exponential resisitivty factor on activation energy, obtained using Efros-Shklovskii's (a) and Mott's (b) law.

spontaneously returned to the pristine HRS state. This state evolved further during long term ageing, as it will be discussed later in the text.

Note that similar spontaneous and current induced metastable states were also observed in LCMO crystals and thin films with other doping levels from the range $0.125 < x < 0.225$ [7–11]. However, among all investigated systems, LCMO crystals doped at $x = 0.14$ show most pronounced differences between HRS and LRS states in the resistivity dependencies on temperature, $\rho(T)$, and current bias, $\rho(I)$. The differences extend into differences in the Meyer-Neldel behavior, as it will be discussed in details further on.

We have fitted the Arrhenius equation (1) to $\rho(T)$ characteristics in Fig. 1, in temperature ranges where the resistivity increases with decreasing temperature, and the local activation energy,

$$E_a(T) = \frac{d[\ln \rho(T)]}{d(1/k_B T)}, \tag{5}$$

remains relatively constant. Figure 2 shows thus obtained logarithm of the pre-exponential factor $\rho_0(T)$ as a function of the local activation energy. The Meyer-Neldel rule predicts that the logarithm of the pre-exponential factor should be a linear function of the activation energy. This behavior is clearly seen in Fig. 2. Data points for $x = 0.3, 0.22, 0.20,$ and 0.18 fall on a single line, meaning that they are characterized by the same Meyer-Neldel temperature T_{MN}. Data for $x = 0.14$ LRS collapse on a line which is slightly shifted with respect to other doping levels, and its slope reveals slightly smaller isokinetic temperature T_{MN}. The data for 0.14 HRS state show also a linear dependence, but markedly separated from the remaining ones, even if the difference between T_{MN} in HRS and LRS state is about the same as the difference between T_{MN} of the LRS and the T_{MN} of stronger doped crystals.

One may raise a question why do we fit the Arrhenius law to our data, while it is known that in the paramagnetic temperature range, charge transport in LCMO is dominated by adiabatic hopping of small polarons [17,18,24–27]. First of all, in one of our publications [7], we have demonstrated, and it was confirmed several times by others [24–26], that $\rho(T)$ data for low-doped manganites in the semiconducting activated regime can be equally well fitted by the Arrhenius law as by the hopping conductivity laws,

$$\rho(T) = \rho_0(T) \exp{(T_0/T)^p}, \tag{6}$$

where T_0 is a characteristic temperature, and the exponent $p = 1$ for nearest-neighbor hopping (NNH), for which the $T_0 = E_a/k_B$. In Mott variable range hopping (VRH) regime, $p = 1/4$ and $p = 1/2$ for Efros-Shklovskii variable range hopping. Secondly, only the detailed differential analysis of the experimental data enables one to find the value of the exponent p and determine which low actually governs the data [24]. Differential analysis of our data indicated that, although in several cases and in limited narrow temperature ranges the exponent corresponded to the Efros-Shklovskii VRH regime, we were not able to univocally determine which hopping law governs the data in the entire investigated temperature and current range.

We have tentatively fitted Eq. (6) with $p = 0.5$ to our $\rho(T)$ data and plotted thus obtained logarithm of the pre-exponential factor as a function of the characteristic temperature in Fig. 3(a). Note that in a difference to Fig. 2, now the data collapse on a single line, with exception of the $x = 0.14$ HRS data that fall on a separate line with a reduced "hopping" isokinetic temperature. However, by fitting Eq. (6) with $p = 0.25$ (Mott's VRH) to the data, the linear fit becomes even better, as can be seen by comparing Figs. 3(a) and 3(b). Upon employing Mott's law, the separation of the HRS data line from the remaining data points is reduced and the very good quality of the linear fit is further increased, as indicated by a slight increase of the Pearson's r factor.

The improved linear behavior of the data upon replacing the activation equation with the Mott's law was previously noted in the literature and led to a claim of existence of a novel hopping Meyer-Neldel rule [28]. It should be underlined that our differential analysis never provided an exponent corresponding to the Mott's regime in any temperature or

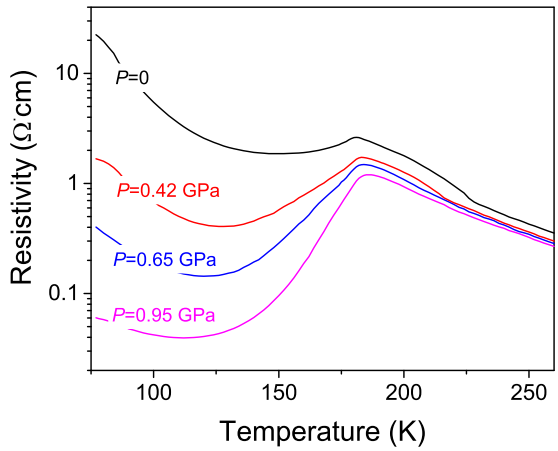

FIG. 4. Temperature dependence of the resistivity of $La_{0.82}Ca_{0.18}MnO_3$ single crystal at different applied hydrostatic pressures.

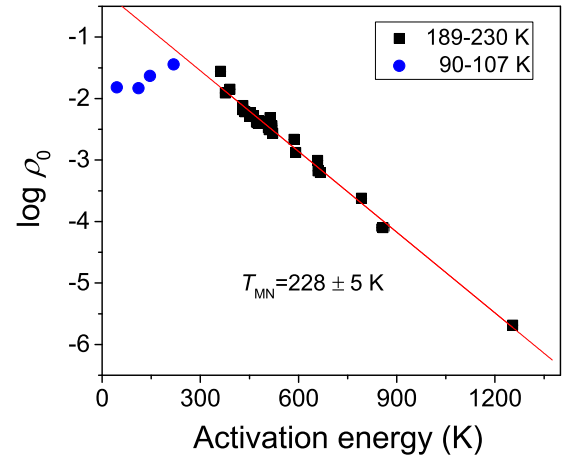

FIG. 5. Dependence of the Arrhenius resistivity pre-exponential factor on the activation energy for data from Fig. 4 at temperatures above (squares) and below T_C (circles).

current range. Moreover, it is easy to verify that the linear fit to the data continuously improves with decreasing value of the exponent p in Eq. (6). Therefore we conclude that the improvement of the linear fit with a hopping law constitutes a simply an artefact related to the compression of scales. Therefore we pursued our analysis using the Arrhenius equation that equally well fits the resistivity data in relatively narrow temperature ranges as the hopping law.

B. Pressure-dependent conductivity

Application of the hydrostatic pressure to LCMO doped below the percolation threshold, $x < 0.225$ leads to changes in the resistivity due to pressure-induced increase of the FMM phase on the expense of the FMI phase [29]. Applied pressure widens the bandwidth of the e_g conduction electrons, which enhances the metallic conductance. Effects of increasing pressure on LCMO resistivity are in fact very similar to the effects of increasing doping.

Figure 4 shows the temperature dependence of the resistivity of a single crystal of $La_{0.82}Ca_{0.18}MnO_3$ at different applied hydrostatic pressure. Pressure application reduces the resistivity, most significantly at $T < T_C$, and widens the temperature range of domination of the FMM phase below T_C. Namely, pressure application shifts the low-temperature resistivity upturn, below which the FMI phase dominates the transport, to lower temperatures. As in the previously discussed case of resistivity influenced by doping, we have fitted the $\rho(T)$ dependencies to Eq. (1) in several temperature ranges in which the resistivity has an activated semiconducting character and the local activation energy remains constant and plotted the logarithm of the pre-exponential factor ρ_0 as a function of the activation energy E_0 in Fig. 5. Again, a Meyer-Neldel behavior of the resistivity varying under applied hydrostatic pressure is revealed. Observe that the Meyer-Neldel isokinetic temperature T_{MN} coincides exactly with the T_{MN} revealed from the doping dependencies of the resistivity in Fig. 2.

For activation energies smaller than about 300 K, corresponding to low temperatures in Fig. 4, the values of the logarithm of ρ_0 deviate from the straight MNR line and even start to decrease in a nonlinear way with decreasing activation energy. Clearly, the MNR behavior breaks down at low activation energies. The reason for this behavior became clear when we have used the records in Fig. 4 to calculate the local activation energy E_a, and plotted it as a function of temperature in Fig. 6.

Above T_C, the local activation energy is almost temperature independent, with exception of the small local maximum associated with the Jahn-Teller transition. With increasing pressure, the maximum decreases and moves towards lower temperatures, consistently with the sharp decrease of the temperature of Jahn-Teller transition with increasing doping [18]. The activation energy of hopping conductivity depends not only on Coulomb and lattice interactions but also on magnetic interactions. The activation energy decreases with temperature decreasing towards T_C due to increase of ferromagnetic correlations. When sample becomes ferromagnetic, spontaneous magnetization appears and gives rise to a sharp decrease of the activation energy. Obviously, negative values of activation

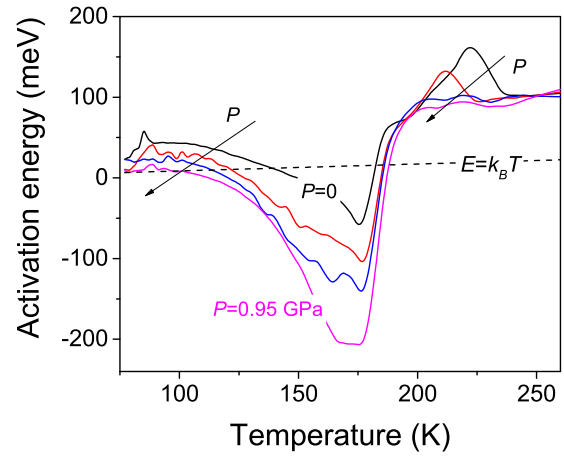

FIG. 6. Local activation energy of $La_{0.82}Ca_{0.18}MnO_3$ single crystal as a function of temperature at various pressures. Arrows indicate the direction of growing pressure.

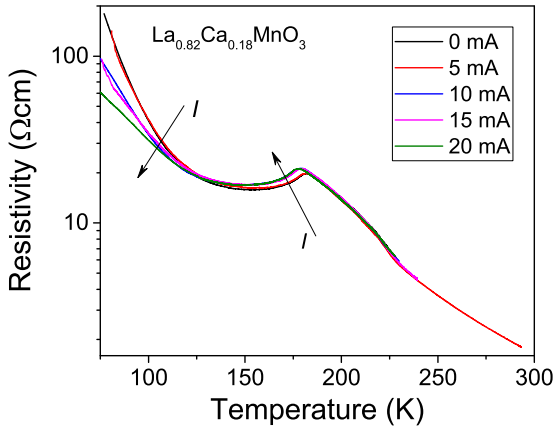

FIG. 7. Temperature dependence of the resistivity of $La_{0.82}Ca_{0.18}MnO_3$ single crystal at different dc bias currents. Arrows indicate the direction of growing current.

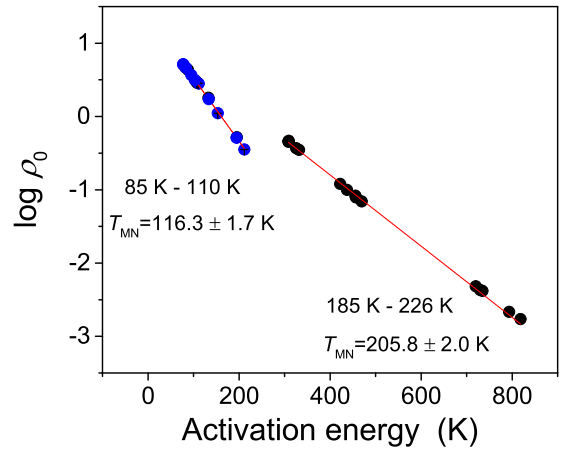

FIG. 8. Dependence of the Arrhenius pre-exponential resistivity factor on the activation energy for data from Fig. 7.

energy at temperature close to T_C are related to the procedure of determining E_a and have no physical meaning.

The necessary condition for appearance of the genuine Meyer-Neldel behavior is the presence of a high energy barrier, $E_a > k_BT$, such that a thermally activated process needs to acquire a big number of individual excitations to overcome the barrier [1]. Comparison of the thermal energy line k_BT with the local activation energy $E_a(T)$ shows that at low temperatures the necessary condition for multiexcitation entropy mechanisms is not fulfilled. Therefore the low-temperature data in Fig. 5 violate the MNR behavior.

C. Current-dependent conductivity

DC current flow is known to influence the resistivity of LCMO crystals and films by inducing metastable resistivity states, or simply reversibly changing the resistance seen under dc current bias [7–9,11,15]. If the current flow influences the resistivity by say, decreasing the activation energy, and the current controlled resistivity follows the Meyer-Neldel rule, then the resistivity will increase with increasing current at temperatures higher than Meyer-Neldel isokinetic temperature T_{MN} and decrease at temperatures $T < T_{MN}$. At $T = T_{MN}$, the resistivity will become current independent.

Figure 7 shows a series of resistivity curves of $La_{0.82}Ca_{0.18}MnO_3$ single crystal recorded under different dc current flow. One can easily see that at low temperatures, below some 120 K, the resistivity is decreasing with increasing current, while for temperatures between 120 K and T_C the increasing current causes resistivity increase.

In order to check whether the resistivity behavior indeed stems from the Meyer-Neldel compensation rule, we again fit Eq. (1) to the activated parts of $\rho(T)$ curves and plot the logarithm of the pre-exponential factor $\rho_0(T)$ as a function of the activation energy in Fig. 8. The plot consists of two linear sections, one coming from the $\rho(T)$ data acquired below T_C, in the 85–110 K range, and the other one, with a higher isokinetic temperature T_{MN}, from the data acquired above T_C, in the range 185–226 K. We note that T_{MN} for the higher temperature range data is very close to the isokinetic temperatures determined from doping and pressure dependencies of the resistivity.

The temperature T_{MN} for the low-temperature range is consistent with the temperature at which $\rho(T)$ curves in Fig. 7 cross and $\rho(T = T_{MN} = 116.3\ \text{K})$ is current-independent, as follows from Eq. (2). Confrontation of the local differential activation energy obtained by differentiating data from Fig. 7 with the k_BT line proves that the necessary conditions for multiexcitation entropy mechanism are fulfilled also in the low-temperature range 85–110 K. One has to accept that there are two distinct isokinetic temperatures, each valid in a separate temperature range. The difference between low- and high-temperature T_{MN} can be attributed to differences in conduction mechanisms above and below T_C. In the higher-temperature range, we deal with small polaron hopping mechanism, while at low temperatures, the conduction is likely dominated by indirect inelastic Glazman-Matveev tunneling mechanism [7].

Note that current-induced changes of the activation energy are markedly different from those imposed by the hydrostatic pressure, compare Figs. 6 and 9. In both cases, the activation energy decreases with increasing pressure or dc current, and the overall shape of $E_a(T)$ dependence is similar. However,

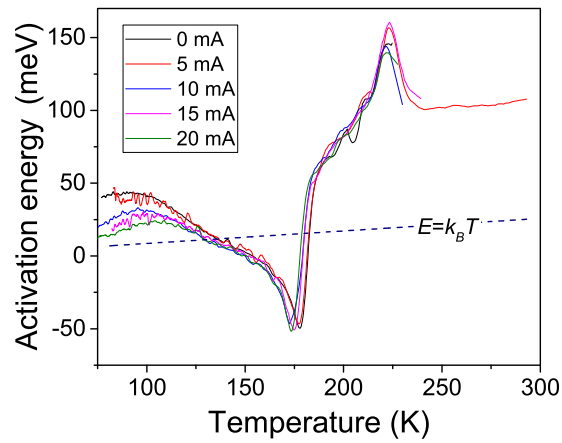

FIG. 9. Apparent activation energy of $La_{0.82}Ca_{0.18}MnO_3$ single crystal as a function of temperature at different currents.

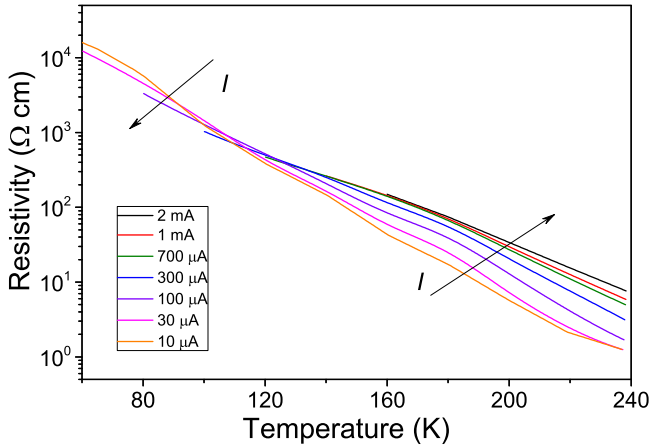

FIG. 10. Temperature dependence of resistivity of $La_{0.86}Ca_{0.14}MnO_3$ single crystal at different dc current bias in the low-resistivity state. Arrows indicate the direction of growing bias current.

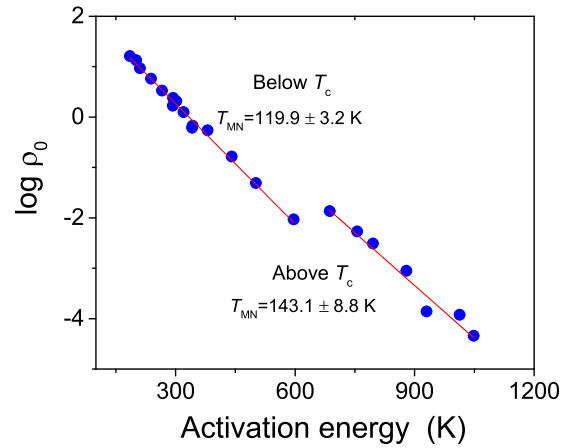

FIG. 11. Dependence of the Arrhenius LRS resistivity pre-exponential factor on the activation energy for data from Fig. 10.

dc current changes the activation energy much weaker than the applied pressure. Moreover, current bias does not change significantly any of the characteristic temperatures, like Jahn-Teller transition temperature or T_C, which are sensitive to the applied pressure. Clearly, current enforced changes of the resistivity are associated with different physical mechanism than the mechanism of pressure induced changes. Applied pressure influences the resistivity by increasing the number of itinerant electrons, what causes an increase of ferromagnetic correlations. Increasing volume of the FMM phase results in a reduction of the energy gap, decrease of the Jahn-Teller transition temperature and shifting of the resistivity upturn point to lower temperatures. The mechanism of current-dependent resistivity in LCMO is not clear yet. One of the plausible scenario may consist in melting of the current driven high-density polarons, accumulating at phase boundaries between metallic and insulating domains, into low density and high-mobility free electrons [30]. However, until now, there is no consensus in the existing literature on the physics behind bias-dependent resistivity of mixed valence manganites.

D. Metastable states and ageing dependent conductivity

The Meyer-Neldel behavior of the current controlled resistance seems to be straightforward evident in the temperature and current dependence of the resistivity of $La_{0.86}Ca_{0.14}MnO_3$ single crystal in the low-resistivity metastable state illustrated in Fig. 10. The experimental $\rho(T)$ characteristics intersect around 120 K. Below this temperature, the resistivity decreases with increasing current, while above 120 K the resistivity increases with increasing current. Such current dependence acts as a positive feedback mechanism in a dynamic current redistribution which results in a generation of robust random telegraph noise in the discussed LCMO single crystals [15].

Fitting of the Arrhenius law to the activated resistivity and plotting thus obtained resistivity pre-exponential factor as a function of the activation energy reveals, as shown in Fig. 11, the existence of two distinct isokinetic temperatures T_{MN}, below and above T_C. The low-temperature $T_{MN} = 119.9 \pm 3.2$ K coincides with the temperature at which the $\rho(T)$ curves intersects, while the slope of linear dependence for the data above T_C reveals $T_{MN} = 143.1 \pm 8.8$ K. The difference between T_{MN} of the low- and high-temperature range can be again attributed to different conductivity mechanisms in high- and low-temperature ranges.

At this point, we want to point out that in a marked difference to LCMO doped at $x = 0.18$, the local activation energy of LCMO doped at the level $x = 0.14$, close to the lower doping limit of the existence of FM ground state, is much more sensitive to the dc current flow, as illustrated in Fig. 12. The activation energy decrease with increasing current, most pronouncedly at higher temperatures above T_C. Namely, at these temperatures, the resistivity increases with increasing current, despite the activation energy decrease, in a spectacular manifestation of the Meyer-Neldel compensation effect.

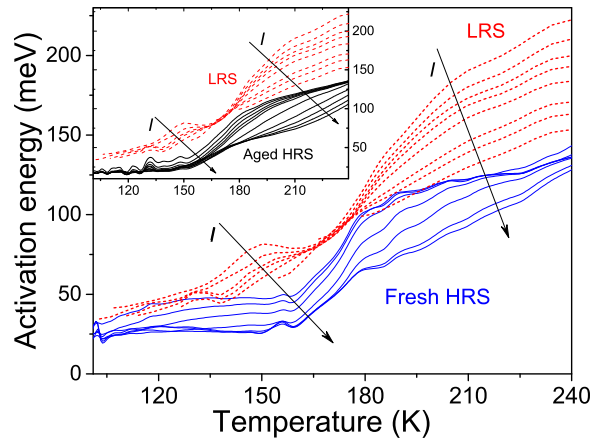

FIG. 12. Temperature dependence of the local activation energy at various bias currents for $La_{0.86}Ca_{0.14}MnO_3$ crystal in LRS (dashed lines) and freshly made HRS state (solid lines). Inset: comparison of the local activation energy of the LRS state (dashed lines) with that of the aged HRS state (solid lines). The arrows indicate the direction of current growth.

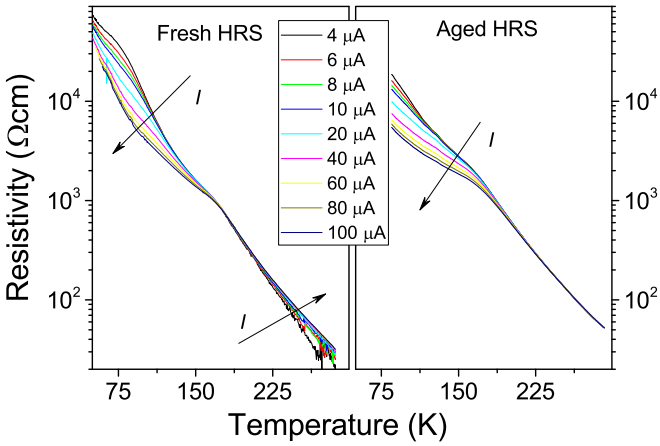

FIG. 13. Temperature dependence of the resistivity of $La_{0.86}Ca_{0.14}MnO_3$ single crystal seen at different dc bias currents in fresh and aged high-resistivity state. Arrows indicate the direction of current growth.

During two-month long break in low-temperature experiments $La_{0.86}Ca_{0.14}MnO_3$ single-crystalline sample spontaneously returned to its pristine high-resistivity state [11]. Since then, the sample never returned to the LRS state but the HRS state was slowly ageing with time. Figure 13 shows the $\rho(T)$ characteristics recorded with various currents for the sample in freshly created HRS and the same characteristics of the HRS state after ageing for almost 3 years.

Figure 13 shows that the temperature at which $\rho(T)$ characteristics intersect, increases upon spontaneous transition of the sample from LRS to the HRS. The T_{MN} increase can be intuitively easily explained under an assumption that ρ_{00} is a constant characterizing given process and does not change upon a transition to different metastable resistivity states. It follows from Eq. (2) that at the isokinetic temperature the resistivity $\rho(T_{MN}) = \rho_{00} = \text{const}$. The fact that HRS resistivity is higher than the LRS resistivity at all temperatures implies that T_{MN} of the higher resistivity state has to be larger than T_{MN} of the lower resistivity state.

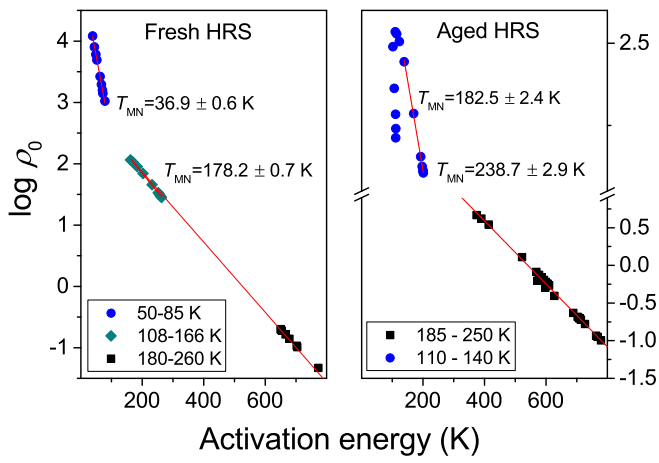

FIG. 14. Dependence of the HRS Arrhenius resistivity preexponential factor on the activation energy for data from Fig. 13.

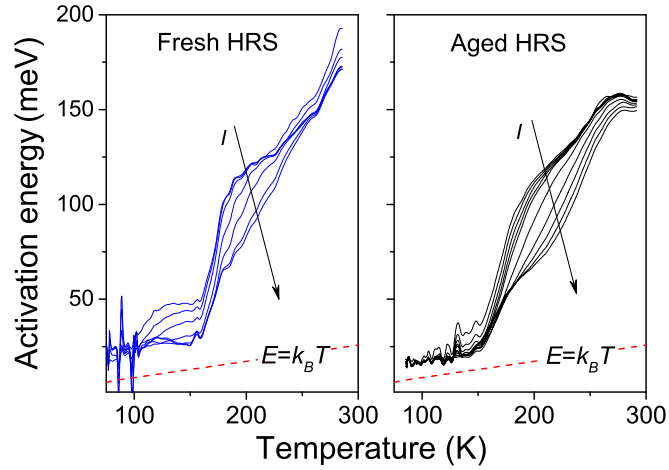

FIG. 15. Temperature dependence of the local activation energy at various bias currents for $x = 0.14$ LCMO sample in fresh HRS and aged HRS state. The arrows indicate the direction of bias current growth.

The isokinetic temperature continues to increase with ageing of the crystal. In the freshly established HRS, the T_{MN} is close to 160 K. In the aged sample, T_{MN} increased so much that the temperature range at which resistivity increases with increasing current is pushed above the room temperature and was not accessed in the experiment.

The quantitative behavior of the isokinetic T_{MN} temperature is revealed using fitting procedures. The results are shown in Fig. 14. Upon a transition from LRS to HRS, the low-temperature range T_{MN} significantly increases from 120 to 163 K. The high-temperature range T_{MN} increases from 143 to 194 K. The HRS resistivity behavior at lower temperatures, below some 85 K, shows yet another $T_{MN} = 37$ K. For the aged sample, the high temperature T_{MN} increases to 239 K, the low-temperature one to 182.5 K, but for temperatures below some 120 K, the Meyer-Neldel behavior of the aged sample breaks down. The data deviate from a straight line and even decrease with decreasing activation energy, as can be clearly seen in Fig. 14. Observe that in the fresh HRS, the MNR holds down to temperatures well below 85 K. Since the local activation energy remains higher than k_BT for fresh and aged metastable states in the entire experimental temperature range, see Fig. 15, one concludes that the break down of the MNR behavior in the aged sample is not associated with violation of the MEE mechanism, as it was in the case of the pressure dependent resistivity, but should be attributed to changes in the conduction mechanism at low temperatures occurring during long ageing of the sample.

IV. CONCLUSIONS

We have shown that the resistivity of low-doped LCMO mangnites influenced by doping, applied pressure, bias current, and ageing time, follows the Meyer-Neldel compensation rule. In the experiments, MNR appears as an insensitivity of the resistance at the temperature corresponding to the isokinetic temperature T_{MN} to any changes in the parameter normally influencing the resistivity. When the isokinetic

temperature falls into the temperature range of the experiment, its reality has been demonstrated directly through intersection of $\rho(T)$ characteristics at this temperature. Alternatively, and more exactly, the T_{MN} was determined through fitting of the activation law to the data and finding the slope of the logarithm of the pre-exponential factor as a function of the activation energy.

Analysis of our experimental results points out that the Meyer-Neldel behavior of LCMO single crystals stems from the multiexcitation entropy mechanism. It is confirmed by the fact that whenever the local activation energy for charge transfer, determined from experimental $\rho(T)$ characteristics, becomes smaller that the thermal energy k_BT, the MNR behavior breaks down. In the light of currently active literature discussion [2–4] on the nature and mechanisms of the compensation phenomenon, we conclude that the compensation effect observed in single-crystalline manganites is a genuine Meyer-Neldel effect, rather than an apparent "compensation behavior" associated with the finite width of the density of states distribution around the Fermi level [2,3]. This is of particular importance since the conductivity of the systems obeying an apparent compensation behavior is in most cases governed by the hopping mechanisms, similarly to the conductivity of manganite crystals in relevant temperature ranges. Nevertheless, it follows that isokinetic temperature in manganite systems has to be determined by the coupling constant N through Eq. (4).

The isokinetic temperature revealed from measurements of differently doped LCMO crystals coincides exactly with the isokinetic temperature determined from the pressure experiments performed with $La_{0.82}Ca_{0.18}MnO_3$ single crystal. This result is consistent with apparent similarity of the mechanisms through which doping and pressure influence the manganite system resistivity. Increasing Ca-doping of LCMO increases the concentration of itinerant electrons and favors the ferromagnetic coupling. Similarly, pressure induces compression of the LCMO crystalline lattice, which increases the Mn-O-Mn bond angle and weakens the electron-lattice coupling [31]. As a result, the overlapping of the (Mn^{3+}) orbitals and the 2p (O^{2-}) orbital enhances the electron hopping rate, which favors charge delocalization and increases ferromagnetic double exchange interactions.

The isokinetic temperatures determined from bias dependent resistivity were found to be different from those following from the pressure and doping experiments. Consistently, the revealed differences in local activation energy dependence on dc current and temperature confirm that mechanisms of current influence upon the LCMO resistivity are different from the pressure and doping based mechanisms. One of the most striking features is the lack of influence of the bias current on the position of Jahn-Teller maximum in the local activation energy.

In general, in current bias experiments, resistivity of $La_{0.82}Ca_{0.18}MnO_3$ and $La_{0.86}Ca_{0.14}MnO_3$ crystals demonstrates different isokinetic temperatures for temperatures below and above T_C. We attribute this fact to different conduction mechanism at low- (ferromagnetic) and high- (paramagnetic) temperature ranges. The low-temperature range isokinetic temperatures T_{MN} for LCMO crystals with markedly different doping levels, $x = 0.18$ and 0.14, seems to be almost the same. At the same time, T_{MN} of $x = 0.18$ doped sample in the paramagnetic range above T_C is higher than that of $x = 0.14$ and much closer to the T_{MN} values revealed from pressure and doping experiments.

The mechanism governing creation and evolution of the metastable resistivity states till today remains obscure. Our experiments reveal that a spontaneous transition from the low-resistivity to high-resistivity state $La_{0.86}Ca_{0.14}MnO_3$ crystal is associated with an increase of the isokinetic temperature. The isokinetic temperature further increases during ageing of the crystal. It seems therefore that the isokinetic temperature can constitute an excellent parameter enabling one to monitor and characterize changes in the conductivity associated with metastable resistivity states. The behavior of the isokinetic temperature can be discussed in terms of differences in the coupling constant N. The physical significance of the coupling constant and its changes can be fully understood only in the framework of a proper microscopic model describing transport governed by multiexcitation entropy in mixed valence manganite systems. Unfortunately, till today such model is not available in the literature. We hope that our experimental results will stimulate future research in that direction.

ACKNOWLEDGMENTS

This work was supported by the Polish NCN Grant 2012/05/B/ST3/03157. The crystals used in the experiments were fabricated by J. Fink-Finowicki in the Institute of Physics, Polish Academy of Sciences in Warsaw and by Ya. Mukovskii in the Moscow State Steel and Alloys Institute.

[1] A. Yelon, B. Movaghar, and R. S. Crandall, Rep. Prog. Phys. **69**, 1145 (2006).
[2] I. I. Fishchuk, A. K. Kadashchuk, J. Genoe, M. Ullah, H. Sitter, T. B. Singh, N. S. Sariciftci, and H. Bässler, Phys. Rev. B **81**, 045202 (2010).
[3] I. I. Fishchuk, A. Kadashchuk, A. Mityashin, M. M. Gavrilyuk, A. Köhler, H. Bässler, J. Genoe, H. Sitter, and N. S. Sariciftci, Phys. Rev. B **90**, 245201 (2014).
[4] A. Yelon, Monatsh. Chem. **144**, 91 (2013).
[5] D. Emin, Phys. Rev. Lett. **100**, 166602 (2008); Monatsh. Chem. **144**, 3 (2013).
[6] J. Hoffmann, P. Moschkau, S. Mildner, J. Norpoth, Ch. Jooss, L. Wu, and Y. Zhu, Mater. Res. Express **1**, 046403 (2014).
[7] Y. Yuzhelevski, V. Markovich, V. Dikovsky, E. Rozenberg, G. Gorodetsky, G. Jung, D. A. Shulyatev, and Y. M. Mukovskii, Phys. Rev. B **64**, 224428 (2001).
[8] V. Markovich, G. Jung, Y. Yuzhelevski, G. Gorodetsky, A. Szewczyk, M. Gutowska, D. A. Shulyatev, and Ya. M. Mukovskii, Phys. Rev. B **70**, 064414 (2004).
[9] V. Markovich, G. Jung, Y. Yuzhelevskii, G. Gorodetsky, F. X. Hu, and J. Gao, Phys. Rev. B **75**, 104419 (2007).

[10] E. Bose, S. Karmakar, B. K. Chaudhuri, and S. Pal, Sol. State Commun. **145**, 149 (2008).
[11] J. Przybytek, J. Fink Finowicki, R. Puźniak, V. Markovich, and G. Jung, J. Appl. Phys. **118**, 043903 (2015).
[12] S. Samanta, A. K. Raychaudhuri, and Ya. M. Mukhovskii, Phys. Rev. B **85**, 045127 (2012).
[13] X. D. Wu, B. Dolgin, G. Jung, V. Markovich, Y. Yuzhelevski, M. Belogolovskii, and Ya. M. Mukovskii, Appl. Phys. Lett. **90**, 242110 (2007).
[14] Y. Yuzhelevski, V. Dikovsky, V. Markovich, G. Gorodetsky, G. Jung, D. A. Shulyatev, and Ya. M. Mukovskii, Fluct. Noise Lett. **01**, L105 (2001).
[15] J. Przybytek, J. Fink-Finowicki, R. Puźniak, A. Shames, V. Markovich, D. Mogilyansky, and G. Jung, Phys. Rev. B **95**, 125101 (2017).
[16] M. Pissas and G. Papavassiliou, J. Phys.: Condens. Matter **16**, 6527 (2004).
[17] E. Dagotto, *Nanoscale Phase Separation and Colossal Magnetoresistance*, Springer series in Solid State Physics (Springer, Berlin 2003).
[18] J. B. Goodenough, in *Handbook on the Physics and Chemistry of Rare Earth*, edited by K. A. Gschneidner, Jr., J.-C. G. Bunzli, and V. Pecharsky (Elsevier Science, New York, 2003), Vol. 33.
[19] R. I. Zainullina, N. G. Bebenin, V. V. Ustinov, Ya. M. Mukovskii, and D. A. Shulyatev, Phys. Rev. B **76**, 014408 (2007).
[20] Y. Tokura, Rep. Prog. Phys. **69**, 797 (2006).
[21] D. Shulyatev, S. Karabashev, A. Arsenov, Ya. Mukovskii, S. Zverkov, J. Cryst. Growth **237-239**, 810 (2002).
[22] E. Rozenberg, M. Auslender, A. I. Shames, G. Gorodetsky, and Ya. M. Mukovskii, Appl. Phys. Lett. **92**, 222506 (2008).
[23] M. Auslender, A. I. Shames, E. Rozenberg, G. Gorodetsky, and Ya. M. Mukovskii, J. Appl. Phys. **105**, 07D705 (2009).
[24] R. Laiho, K. G. Lisunov, E. Lähderanta, V. S. Stamov, V. S. Zakhvalinskii, Ph. Colomban, P. A. Petrenko, and Yu. P. Stepanov, J. Phys.: Condens. Matter **17**, 105 (2005).
[25] R. Laiho, K. G. Lisunov, E. Lähderanta, V. S. Stamov, and V. S. Zakhvalinskii, J. Phys.: Condens. Matter **13**, 1233 (2001).
[26] N. G. Bebenin, R. I. Zainullina, N. S. Chusheva, V. V. Ustinov, and Ya. M. Mukovskii, J. Phys.: Condens. Matter **17**, 5433 (2005).
[27] P. Dai, J. A. Fernandez-Baca, N. Wakabayashi, E. W. Plummer, Y. Tomioka, and Y. Tokura, Phys. Rev. Lett. **85**, 2553 (2000).
[28] N. P. Reddy, R. Gupta, and S. C. Agarwal, J. Non-Cryst. Solids **364**, 69 (2013).
[29] V. Markovich, I. Fita, E. Rozenberg, R. Puźniak, D. Mogilyansky, A. Wisniewski, Ya. M. Mukovskii, G. Gorodetsky, J. Magn. Magn. Mater. **264**, 70 (2003).
[30] D. Emin, Phys. Rev. B **74**, 035206 (2006).
[31] P. G. Radaelli, G. Iannone, M. Marezio, H. Y. Hwang, S.-W. Cheong, J. D. Jorgensen, and D. N. Argyriou, Phys. Rev. B **56**, 8265 (1997).